Bragg Scattering from Atoms in Optical Lattices

G. Birkl, M. Gatzke, I. H. Deutsch, S. L. Rolston, and W. D. Phillips
National Institute of Standards and Technology, PHYS A167, Gaithersburg, Maryland 20899
(Received 14 June 1995)

We observe coherently enhanced reflection (Bragg scattering) of a near resonant laser beam from cesium atoms ordered by a periodic array of optical potential wells known as an optical lattice. The reflected light is enhanced by a factor of $\sim 10^5$ over scattering from a disordered atomic sample. We measure the magnitude of the reflectivity and its detuning dependence as functions of the density and the degree of localization of the atoms. The change in lattice constant due to the frequency-dependent effective index of refraction seen by the lattice light field is observed.

PACS numbers: 42.25.Bs, 32.80.Pj

Optical lattices are periodic light-shift potentials for atoms, created by the interference of multiple laser beams. In these light fields, atoms are laser cooled and localized at the potential minima with spatial extents smaller than the wavelength of the lattice light [1–3]. We reflect (Bragg scatter) a laser beam from the atomic sample to probe the long-range periodic order of the atoms. In contrast to previous nonlinear wave mixing experiments [4–6], we scatter probe light only after the lattice beams are turned off. This avoids any contribution from lattice light scattered from atomic polarization gratings formed by the interference of lattice and probe waves. In principle, our experiment is identical to x-ray diffraction experiments demonstrating periodicity in solid-state crystals. However, the optical lattice constants are on the order of a micron rather than an angstrom, and therefore Bragg scattering occurs at optical wavelengths.

Our three-dimensional optical lattice for Cs atoms is created by the interference of two pairs of linearly polarized laser beams as shown in Fig. 1 [7,8]. The lattice beams have a diameter of about 10 mm, a uniform intensity, typically 1 mW/cm^2, and a typical detuning of five natural linewidths ($\Gamma/2\pi = 5.2$ MHz) below the $6S_{1/2}(F = 4) \rightarrow 6P_{3/2}(F' = 5)$ transition at $\lambda_L = 852$ nm. The resulting light field has points of pure σ^+ and σ^- polarization (with respect to z), each arranged as a centered tetragonal lattice, with a spacing between sites of opposite polarization of approximately $\lambda_L/2\sqrt{2}$ along z and $\lambda_L/\sqrt{2}$ along x and y. Atoms are cooled and trapped at these sites, where they are optically pumped predominately into the states $F = 4$, $m_F = \pm 4$, respectively. The loss of atoms to the $F = 3$ ground state is prevented by a repumping laser, left on continuously.

The condition for Bragg scattering requires that the difference in wave vectors between an incident probe and a reflected wave be a reciprocal lattice vector of the periodic potential. In optical lattices, a basis for the reciprocal lattice is formed by the differences between the wave vectors of the lattice laser beams [9]. In order to make use of a resonantly enhanced scattering cross section, we tune the probe laser near the same atomic transition used to create the lattice. At this probe wavelength, only first order Bragg scattering is allowed, for which there are twelve possible directions of the incident probe beam (eight collinear with lattice beams, and four in the x-y plane). We use the geometry shown in Fig. 1, where the probe beam is counterpropagating against one of the lattice beams, and is reflected from planes of atoms into directions counterpropagating against the other three lattice beams. We detect only the beam that is reflected from Bragg planes normal to x, which have a spacing of $\lambda_L'/\sqrt{2}$. Because of the dispersive interaction with the atoms, the wavelength of the lattice beams inside the medium, λ_L', deviates from the vacuum wavelength λ_L. The difference is small (less than 10^{-3}) but nonetheless has effects which we have measured.

In a 4 ms cycle, we load our optical lattice with Cs atoms collected in a magneto-optical trap (2 ms) then cooled in an optical molasses (1 ms) as described in Ref. [8]. The molasses beams are shut off and the atoms are allowed to equilibrate in the lattice for 1 ms, reaching temperatures of about 10 μK. This produces a dense (several 10^{10} cm^{-3}) sample of atoms in a volume of about 0.2 mm^3 having about 2000 Bragg planes normal to x. Even at a density of $n_0 = 9 \times 10^{10}$ cm^{-3} only

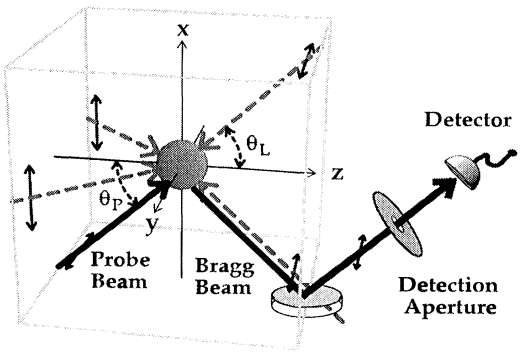

FIG. 1. Configuration of laser beams creating a three-dimensional optical lattice, together with the directions of probe beam and Bragg scattered beam ($\theta_L \approx \theta_P \approx 45°$).

1 in 100 lattice sites would be occupied. The cycle is completed when the lattice is turned off (switching time ~100 ns) and the probe is introduced. Typically, the turn-on of the probe is delayed by about 100 ns with respect to the turn-off of the lattice, long enough that the lattice light is completely extinguished, but short enough that the atoms do not move significantly. The probe beam is applied for about 0.5 μs and has a typical intensity of 0.03 mW/cm^2. At this low intensity the motion of the atoms is not significantly altered by photon recoil and almost all light is scattered elastically (i.e., into the "δ-function" component of the fluorescence spectrum). The reflected light is split off from the lattice beam direction by a beam splitter, sent through a spatial filter, and detected by a photomultiplier tube (Fig. 1). The total solid angle of detection, 4.1×10^{-4} sr, is defined by a circular aperture with a full angular opening of 23 mrad.

The polarization of the probe light can be chosen freely, but is linear along y for most of our experiments, maximizing the reflectivity. For this polarization, which can be decomposed into σ^+ and σ^- with respect to z, atoms in the $m_F = \pm 4$ ground states have equal scattering cross sections, with $m_F = +4$ ($m_F = -4$) atoms scattering mostly σ^+ (σ^-) light. Since the Bragg planes contain an equal number of $m_F = \pm 4$ atoms, the polarization of the reflected beam we observe is the same as that of the probe. Changing the probe polarization to either helicity of circular polarization reduces the intensity of the Bragg reflected light by a factor of 2. Keeping the polarization linear, but rotating it by 90° so that it lies in the plane of incidence, decreases the reflectivity by more than a factor of 15. This large reduction occurs because, for this geometry and polarization, a generalized condition for Brewster's angle is nearly satisfied.

By comparing the amount of scattered light from an ordered and a disordered (no lattice beams applied) atomic sample, we directly determine the coherent enhancement for light reflected along a Bragg direction. We find an increase in the on-axis intensity of the Bragg scattered beam of $\sim 10^5$ and the maximum reflectivity of (0.35 ± 0.15)%, at a probe detuning of about 1Γ. For a disordered atomic sample, the angular distribution of scattered light is uniform across our 23 mrad detection aperture. By contrast, the Brag reflected beam has a Gaussian profile with a full width at half maximum of 1.34 ± 0.10 mrad. This divergence is consistent with the estimated ~1 mrad diffraction angle due to the size of the atomic sample. We estimate the probe acceptance angle for Bragg scattering, inversely proportional to the number of planes, to be less than 0.5 mrad. Because the divergence of the probe beam (1.5 ± 0.2 mrad) is larger than this acceptance angle, we expect the observable reflectivity to be reduced.

At the moment the lattice turns off ($t = 0$), we expect approximately Gaussian distributions for both the position and momentum of the atoms in each plane [10]. The position spread reduces the strength of the reflected signal by $\beta = \exp[-K^2 \Delta x^2(t)]$ (the Debye-Waller factor of x-ray crystal diffraction [11]), where $\Delta x^2(t)$ is the mean squared position spread (localization), $K = \sqrt{2}\, k$ is the momentum transfer for Bragg scattering in our geometry, and $k = 2\pi/\lambda_L$. The atoms are initially localized to $\sim \lambda/7$ ($\beta \sim 0.2$), independent of their temperature [10,12]. The momentum spread leads to an increasing position spread with time, and therefore to a temporal decay of the Bragg reflectivity after the lattice is shut off. We observe this by measuring the reflectivity as a function of probe delay. Figure 2 shows two decay curves well fit by $I(t) = I(0)\exp(-t^2/2\tau^2)$ with decay constants $\tau = 2.0 \pm 0.1$ and 1.6 ± 0.1 μs. The temperatures for these curves, measured independently by a time-of-flight method [8], are $T = 8.5 \pm 1$ and 14.0 ± 1 μK, respectively. Using these temperatures and the time-dependent Debye-Waller factor β with $\Delta x^2(t) = \Delta x^2(0) + \langle p_x^2 \rangle t^2/m^2$ and $\langle p_x^2 \rangle/m = k_B T$, we predict decay constants of $\tau = 3.0 \pm 0.2$ and 2.1 ± 0.1 μs, respectively. Although the predictions and the experimental values differ by about 30%, the measurements demonstrate the reduction in reflectivity due to the decrease in localization. The temporal decay in reflectivity cannot be attributed to the loss of atoms as they fall out of the probe beam, which occurs on the much longer time scale of 10 ms.

In order to investigate the competition between Bragg and diffuse scattering, we study the probe-detuning dependence of the reflectivity for Bragg scattering (reflection spectrum) for various densities. Figure 3 shows a series of reflection spectra for densities at the center of the sample ranging from $n_0 = 3 \times 10^9$ to 8×10^{10} cm^{-3}. The densities are determined from the transmission of the probe beam, accounting for the beam profile and the Gaussian density distributions across the sample. The absolute uncertainties in the measured densities are estimated to be 25% with a relative uncertainty of 5% be-

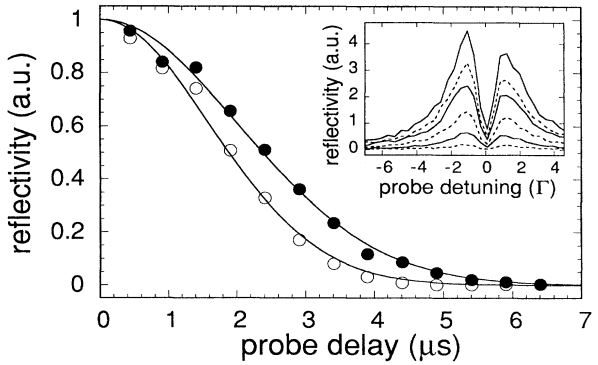

FIG. 2. Reflectivity as a function of the time delay of the probe pulse for two different atomic temperatures: (•) $T = 8.5$ μK and (○) $T = 14.0$ μK. A lower temperature leads to a longer decay time. The inset shows reflection spectra for time delays from 0.1 to 4.6 μs. The shape of the spectrum does not change with increasing time (i.e., decreasing localization).

tween the different measurements shown in Fig. 3. For low densities ($n_0 = 3 \times 10^9$ cm^{-3}) the reflection spectrum is well fit by a Lorentzian with a width of 1.4Γ. This width is consistent with the natural linewidth Γ and the ~2 MHz frequency jitter of the probe laser. Besides the strong enhancement of the reflectivity, this spectrum is identical to that from a sample of disordered atoms; i.e., the shape is determined solely by the absorption cross section. For increasing densities the spectra become broader and develop a flat top ($n_0 = 2 \times 10^{10}$ cm^{-3}) and eventually a dip around atomic resonance for the highest densities ($n_0 = 4 \times 10^{10}$ and 8×10^{10} cm^{-3}). The symmetry of the spectra is very sensitive to the relative alignment of probe and lattice beams, as discussed below. For the data presented in Fig. 3, the alignment was chosen to produce symmetric spectra.

The inset in Fig. 3 shows a set of calculated reflection spectra, based on a simplified model, but accounting for diffuse scattering loss and scattering phase shifts. Given our density and small Debye-Waller factor ($\beta \sim 0.2$), the specular reflectivity per plane is much smaller than the diffuse scattering loss per plane [13]. Under these conditions, we can neglect multiple reflections (i.e., we consider interference of those waves which have been specularly reflected only once from the various planes), in contrast to the model used in Ref. [14].

Diffuse scattering loss is significant and leads to frequency dependent attenuation of the probe and reflected waves as determined by the absorption cross section (only 3% of the probe light is transmitted at resonance for $n_0 = 8 \times 10^{10}$ cm^{-3}). The effective number of planes contributing to Bragg scattering is therefore detuning dependent, substantially reducing the reflectivity near resonance when the sample is optically thick. Thus the reflectivity in the wings of the spectra grows faster with density than at resonance, causing the spectra to broaden and to develop a dip [15]. In the limit of low reflectivity, the atomic localization on the other hand does not affect the shape of the spectra but simply determines the magnitude of the reflectivity according to the Debye-Waller factor [16]. This is illustrated in the inset in Fig. 2 by a series of experimental reflection spectra at constant density for increasing probe delay (i.e., increasing position spread), which show a decreasing reflectivity but constant shape.

The reflection spectra are affected not only by absorption but also by dispersion of the probe. Furthermore, dispersion of the lattice beams causes the lattice constant d to be a function of lattice laser frequency ω_L. For our configuration (Fig. 1), $d = \lambda_L/2n_{\text{eff}}(\omega_L)\sin\theta_L$, where $n_{\text{eff}}(\omega_L)$ is the effective index of refraction seen by the lattice light field at the frequency ω_L [14]. Through the lattice constant d the Bragg condition $2d\sin\theta_P = \lambda_P/n(\omega_P)$ depends on the lattice frequency as well as on the angle $\Delta\theta = |\theta_L - \theta_P|$ between the lattice and probe [17]. Here λ_P is the probe vacuum wavelength, and $n(\omega_P)$ is the usual index of refraction for an atomic gas near resonance. The Bragg condition is exactly satisfied for a probe on atomic resonance [$n(\omega_P) = 1$] when we choose $\Delta\theta = \Delta\theta_{\text{sym}}(\omega_L) = n_{\text{eff}}(\omega_L) - 1$ [16]; for this choice, we expect symmetric reflection spectra, such as shown in Fig. 3. For our range of experimental parameters, $\Delta\theta_{\text{sym}}(\omega_L) \leq 1$ mrad. For $\Delta\theta \neq \Delta\theta_{\text{sym}}$, the Bragg condition is satisfied off-resonance, leading to asymmetric spectra (see inset in Fig. 4).

We use the relationship between the symmetry of the spectra and the difference angle $\Delta\theta$ to determine the change in lattice constant as a function of lattice frequency. From the Bragg condition and the expression

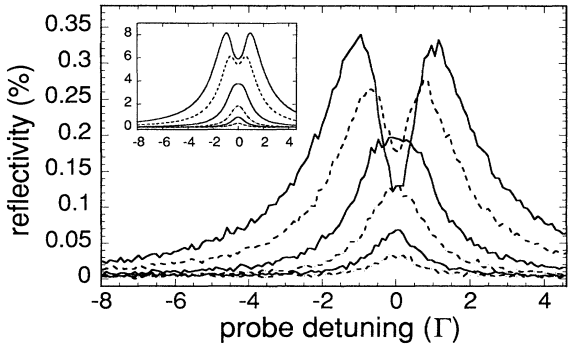

FIG. 3. Bragg reflectivity as a function of probe laser detuning for densities from 3×10^9 to 8×10^{10} cm^{-3}, increasing by roughly a factor of 2 between traces. For increasing densities, the spectra become broader and develop a dip at resonance. The temperature of the atoms is $T = 12$ μK and the initial localization is $\sim \lambda/7$. The inset (same axes) shows calculated reflection spectra for the same parameters in a one-dimensional model, neglecting some experimental details such as the shape of the sample, the probe beam profile, and the probe divergence.

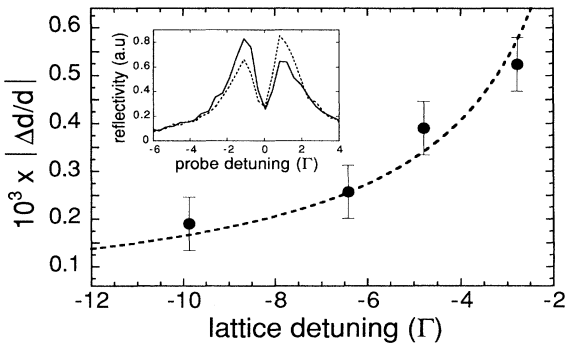

FIG. 4. Fractional change in lattice constant $\Delta d/d$ as a function of lattice laser detuning (•) together with a calculation based on the experimental values for atomic density and localization (dashed line). The measurement of $\Delta d/d$, plotted with a fitted offset, is based on determining the angle between the lattice and probe beams necessary to produce symmetric spectra. The inset shows asymmetric reflection spectra for different choices of this angle.

for d given above, with $\theta_L \approx \theta_P \approx 45°$, one can derive the relation $|\Delta d/d(\omega_L)| = n_{\text{eff}}(\omega_L) - 1 = \Delta\theta_{\text{sym}}(\omega_L)$, where Δd is the change in lattice constant relative to the case of $n_{\text{eff}}(\omega_L) = 1$. For various values of ω_L we adjust the beam alignment to produce symmetric spectra and measure $\Delta\theta_{\text{sym}}(\omega_L) = |\Delta d/d(\omega_L)|$ relative to the fixed but unknown offset $\Delta\theta_{\text{sym}}(-9.8\Gamma) = |\Delta d/d(-9.8\Gamma)|$. We must introduce this offset because the absolute angle between lattice and probe beams cannot be measured with the necessary accuracy. Figure 4 shows a calculation of $\Delta d/d$ for a density of $n_0 = 3 \times 10^{10}$ cm^{-3} and a localization of $\lambda/7$. The $\Delta d/d$ measured for these experimental parameters is plotted with an offset to give the best fit to theory. The error bars represent the uncertainty in determining when the spectrum is exactly symmetric. Because optical lattices are self-organizing such that the standing wave lattice light field has the same periodicity as the dielectric medium, the effective index of refraction $n_{\text{eff}}(\omega)$ for the standing wave is different from the usual index $n(\omega)$ for a traveling wave. For perfect atomic localization, $n_{\text{eff}}(\omega_L) - 1 = 4[n(\omega_L) - 1]$. In general, the finite position spread gives the result $n_{\text{eff}}(\omega_L) - 1 = (1 + 3\sqrt{\beta})[n(\omega_L) - 1]$ [16], where β is the Debye-Waller factor defined above. The observed detuning dependent change in lattice constant is evidence for the backaction of the dispersive medium on the optical lattice light field, although for our Debye-Waller factor ($\beta \sim 0.2$), uncertainties in the measured values of density and $\Delta d/d$ prevent us from unambiguously verifying the correction factor $3\sqrt{\beta}$ experimentally.

We have demonstrated Bragg scattering as a new tool complementing probe-absorption spectroscopy and fluorescence spectroscopy for investigating optical lattices. With this technique we should be able to study important properties of atoms in optical lattices such as the fraction of atoms which are trapped and ordered. Future improvements in localization and density will allow us to measure unambiguously the modification of the index of refraction for standing waves in a periodic medium. Furthermore, we can enter a regime where multiple reflections become important and possibly observe such phenomena as photonic band gaps [18] and photon localization [19].

We gratefully acknowledge helpful discussions with T. B. Lucatorto and A. Steinberg. This work was made possible in part by the U.S. Office of Naval Research and through NSF Grant No. PHY-9312572. G. B. thanks the Alexander von Humboldt Foundation for financial support.

[1] P. Verkerk *et al.*, Phys. Rev. Lett. **68**, 3861 (1992).
[2] P. S. Jessen *et al.*, Phys. Rev. Lett. **69**, 49 (1992).
[3] A. Hemmerich and T. W. Hänsch, Phys. Rev. Lett. **70**, 410 (1993).
[4] B. Lounis *et al.*, Europhys. Lett. **21**, 13 (1993).
[5] G. Grynberg *et al.*, Phys. Rev. Lett. **70**, 2249 (1993).
[6] A. Hemmerich, M. Weidemüller, and T. W. Hänsch, Europhys. Lett. **27**, 427 (1994).
[7] P. Verkerk *et al.*, Europhys. Lett. **26**, 171 (1994).
[8] A. Kastberg *et al.*, Phys. Rev. Lett. **74**, 1542 (1995).
[9] K. I. Petsas, A. B. Coates, and G. Grynberg, Phys. Rev. A **50**, 5173 (1994).
[10] S. Marksteiner *et al.*, Appl. Phys. B **60**, 145 (1995).
[11] See, for example, N. W. Ashcroft and N. D. Mermin, *Solid State Physics* (Saunders, Philadelphia, 1976), Chap. 6 and App. N.
[12] M. Gatzke, G. Birkl, P. S. Jessen, A. Kastberg, W. D. Phillips, and S. L. Rolston, (to be published).
[13] Because of the low filling fraction there are large density fluctuations within each plane. Together with the finite position spread of the atoms normal to the planes, described by the Debye-Waller factor, this causes the scattering to be predominately diffuse (i.e., into non-Bragg directions).
[14] I. H. Deutsch *et al.*, Phys. Rev. A **52**, 1394 (1995).
[15] The observed reflectivity at resonance actually decreases at the highest densities, in contrast to the calculated spectra shown in the inset of Fig. 3. A preliminary calculation including a small number of disordered atoms qualitatively reproduces this feature and reduces the discrepancy between the magnitudes of the calculated and observed reflectivities. We attribute the remaining discrepancy in part to the use of a probe beam with a divergence larger than the acceptance angle.
[16] I. H. Deutsch, G. Birkl, M. Gatzke, W. D. Phillips, and S. L. Rolston (to be published).
[17] The probe-frequency dependence of the Bragg condition is determined almost entirely by the variation of $n(\omega_p)$ rather than the direct variation in the vacuum wavelength λ_P ($\Delta\lambda_P/\lambda_P \sim 10^{-8}$ over the width of the reflection spectra).
[18] See J. Opt. Soc. Am. B **10**, No. 2 (1993), special issue on photonic band gaps, edited by C. M. Bowden, J. P. Dowling, and H. O. Everitt.
[19] S. John, Phys. Today **44**, No. 5, 32 (1991).